applied sciences

MDPI

Article

Analysis of the Effect of Antenna Pointing Error Caused by Satellite Perturbation on Space Terahertz Communication

Yuanzhi He * and Chensheng Ma

Academy of Military Sciences, Institute of Systems Engineering, Beijing 100141, China
* Correspondence: he_yuanzhi@126.com

Abstract: The terahertz frequency band has the advantages of having a large bandwidth, narrow beam, strong penetration, and high security, and is an important direction for the frequency expansion of next-generation satellite communications. Due to the narrow terahertz beam, the pointing error caused by satellite perturbation will affect the attenuation of the terahertz wave power, resulting in a decrease in the received power of the system and affecting the communication performance of the system. In order to accurately analyze the influence of pointing error caused by satellite perturbation on the performance of space terahertz communication system, based on satellite perturbation model and Gaussian channel model, this paper deduces the accurate analysis of signal power attenuation model without pointing error and with pointing error untie. The antenna pointing error in the real environment is simulated by using the TLE data of the actual satellite, and the influence of the pointing error on the space terahertz communication is analyzed. The results show that the antenna pointing error caused by satellite perturbation changes periodically with the operation of the satellite, which will cause great signal power attenuation, reduce the signal-to-noise ratio of the space terahertz communication system, and seriously affect the communication quality. In addition, the higher the frequency, the greater the impact on space terahertz communication, which needs to be solved through attitude control and antenna compensation.

Keywords: satellite perturbation; pointing error; Gaussian channel model; terahertz communication

check for updates

Citation: He, Y.; Ma, C. Analysis of the Effect of Antenna Pointing Error Caused by Satellite Perturbation on Space Terahertz Communication. *Appl. Sci.* **2022**, *12*, 10772. https://doi.org/10.3390/app122110772

Academic Editors: Houjun Sun, Hua Qin and Yu Xiao

Received: 22 September 2022
Accepted: 21 October 2022
Published: 24 October 2022

Publisher's Note: MDPI stays neutral with regard to jurisdictional claims in published maps and institutional affiliations.

Copyright: © 2022 by the authors. Licensee MDPI, Basel, Switzerland. This article is an open access article distributed under the terms and conditions of the Creative Commons Attribution (CC BY) license (https://creativecommons.org/licenses/by/4.0/).

1. Introduction

With the development of satellite communication technology, the contradiction between the supply and demand of spectrum resources has become more and more serious, and it has become a scarce strategic resource. In recent years, the terahertz frequency band, which is higher than microwave, has become a research hotspot all over the world. With the rapid development of terahertz communication technology, China, Germany, Japan, France, the United States, and other countries have successfully carried out terahertz communication system tests [1–5]. The terahertz frequency band is between the relatively mature microwave frequency band and the infrared frequency band. It has special characteristics. It has both the excellent characteristics of microwave and laser, and has the unique advantages of large bandwidth, narrow beam, strong directivity and so on. However, its molecular absorption characteristics in the atmosphere are relatively obvious. Therefore, for satellite communication, its main application scenario is inter-satellite communication. Due to the high frequency of terahertz waves, the beam angle is narrower than that of microwaves, and direct intensity modulation is generally used in satellite communication systems, which leads to an increase in the bit error rate. The performance of inter-satellite terahertz communication systems is easily restricted by many factors such as pointing error.

From a macro perspective, the satellite orbit is fixed, and the antenna pointing tracking between satellites can be accurately calculated according to the orbit parameters. However, the actual situation is that satellites are always affected by various perturbations of the space environment, including the additional gravitational force generated by the non-spherical

shape of the Earth and uneven mass, the gravitational force of the sun, the moon and other celestial bodies, atmospheric resistance, solar light pressure, etc. Under the action of the perturbation force, the orbit and attitude of the satellite are constantly changing, which will cause the deviation of the pointing of the terahertz antenna to produce pointing errors, thus affecting the performance of the terahertz communication system. Reference [6] studied the relative motion between a pair of small satellites during formation flying and proposed a model for orbital perturbation caused by gravitational force, the Earth's oblateness, and solar radiation pressure. They prove that the relative motion of satellites is bounded, which provides a theoretical foundation to characterize the beam misalignment using a Gaussian distribution. Reference [7] uses STK to simulate the link model in the terahertz space application scenario, and analyzes the requirements of the space terahertz communication link for the terahertz wave pointing accuracy. In reference [8], based on the technical requirements of inter-satellite terahertz communication application and the existing high-gain antenna, the demand of acquisition pointing tracking (APT) technology in terahertz communication system are analyzed. By simulating the tracking and pointing error of the APT subsystem, it is found that the tracking and pointing error has an important influence on the received power of the communication system. Through simulation calculation, the influence of satellite platform vibration on terahertz communication is analyzed. When the frequency is 0.34 THz, there is almost no effect on THz communication, and when the frequency increases to 1.5 THz and above, the effect becomes larger. The above literature only analyzes the pointing accuracy requirements and the impact of the pointing error caused by the vibration of the satellite platform on the received power, but does not specifically analyze the pointing error caused by the satellite perturbation. At the same time, there are few studies on the antenna pointing errors caused by perturbation to satellites in different orbits. In this paper, the perturbation model and pointing error model are established by analyzing the specific perturbation force of the satellite and the specific direction of the antenna during the orbit, and based on the established model, the influence of the pointing error generated by the satellite perturbation on the terahertz communication system is analyzed.

In the Section 2 of this paper, the perturbation forces of the satellite in different orbits are analyzed. The perturbation forces with less influence are ignored, and the ones with more influence are selected for research. Then the satellite perturbation model is established by solving the satellite perturbation motion based on the existing satellite motion equation and perturbation force research. In the Section 3, the terahertz communication system model and noise model are introduced. In the Section 4, the terahertz wave is modeled as Gaussian beam by referring to the processing method of optical band pointing error, and the exact analytical solutions of the signal power attenuation model are derived in the case of no pointing error and with pointing error. In the Section 5, according to the two-line element (TLE) data of the actual satellite, the simulation results in the real space terahertz communication scenario are given, and the influence of the antenna pointing error caused by the satellite perturbation on the space terahertz communication is analyzed.

2. Satellite Perturbation Model

The motion of a satellite around the Earth is the subject motion under the action of the gravity of the center of the Earth and various perturbation forces in space, and its orbit is not static, as shown in Figure 1. Although the magnitude of these perturbations is small compared to the central gravity of the Earth, they also have certain effects on satellite orbits. Correspondingly, it has a huge impact on the pointing of narrow beam terahertz antennas in high frequency bands. The perturbation force is usually divided into two types: conservative force and non-conservative force. Among them, the conservative force is only related to the orbital position of the satellite; the non-conservative force has complex influence factors and is also related to the speed of the satellite and the surface characteristics of the star. Conservative forces include Earth's non-spherical gravitation, N-body gravitation (sun, moon, and other planets), solid tide perturbation, ocean tide

perturbation, etc. Non-conservative forces include solar pressure, atmospheric drag, and Earth's albedo pressure. These perturbation forces cause different perturbation accelerations to satellites at different orbital altitudes, and have different effects on pointing errors. Therefore, to establish a perturbation model for satellites in different orbits, it is necessary to analyze the specific requirements and make a reasonable choice of various perturbation forces. Figure 2 shows the influence of the main perturbation force on the acceleration of low-orbit (LEO, 200–2000 km), medium-orbit (MEO, 2000–20,000 km) and geostationary orbit (GEO, 35,786 km) satellites, reflecting the influence of different perturbation forces on the motion of satellites at different altitudes.

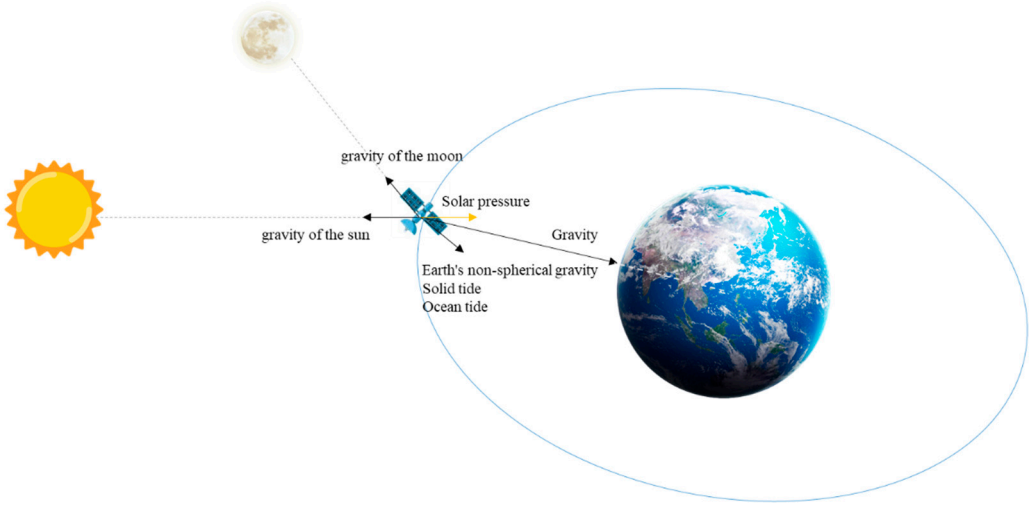


Figure 1. The orbital perturbation model of satellites under the factors of third-body gravity, non-uniform gravity, and light pressure.

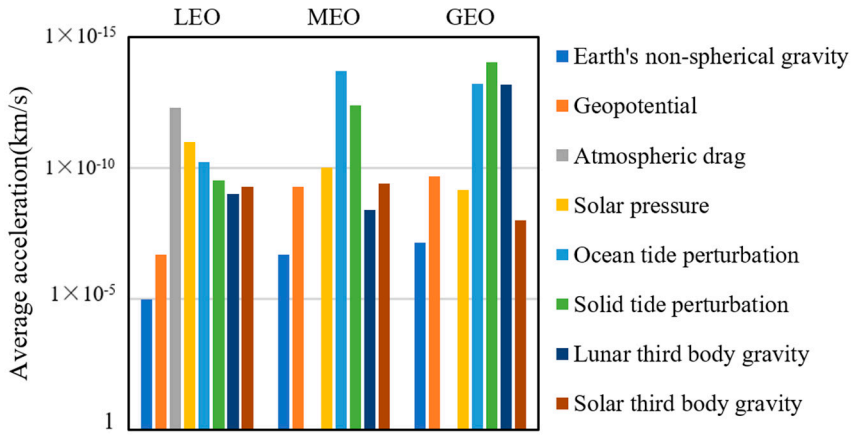


Figure 2. The magnitude of the perturbation force on satellites in different orbits.

In addition to the central gravity of the earth, low-orbit satellites also need to consider high-order aspheric gravity of the Earth, atmospheric drag, sun-moon gravity, tidal perturbation, and solar light pressure. Due to the high orbital height of geostationary orbit satellites, atmospheric resistance will not affect them, and it is mainly necessary to consider the aspheric gravity of the Earth, the gravity of the sun and the moon, and the solar light pressure, etc.

Generally speaking, the motion equation of the satellite photographed motion can be expressed as Equation (1).

$$\ddot{\vec{r}} = \vec{a}_g + \vec{a}_{ng} = \left(-\frac{GM_e}{r^3}\vec{r} + \frac{\vec{F}_{pot} + \vec{F}_{slb} + \vec{F}_{dt} + \vec{F}_{ot}}{m} \right) + \frac{\vec{F}_{sp} + \vec{F}_{dp}}{m} \quad (1)$$

Among them, $\vec{r}$ is the position of the satellite in the inertial coordinate system, $\vec{r} = (x, y, z)^T$; $\vec{a}_g$ is the sum of the conservative forces acting on the satellite; $\vec{a}_{ng}$ is the sum of the non-conservative forces acting on the satellite surface; GM_e is the gravitational constant of the Earth; $\vec{F}_{pot}$ is the perturbation force of the Earth's gravitational field; $\vec{F}_{slb}$ is the gravitational perturbation of the sun, moon, and other planets; $\vec{F}_{dt}$ is the solid tide perturbation; $\vec{F}_{ot}$ is the ocean tide perturbation; $\vec{F}_{sp}$ is the solar light pressure perturbation; $\vec{F}_{dp}$ is the Earth's atmospheric resistance perturbation.

For the convenience of solving, the equation of motion is usually transformed into a first-order differential equation, and then the variational equation is solved by numerical integration method according to the initial parameters of the satellite orbit. In this paper, the initial parameters of the satellite orbit are obtained by the two-line element (TLE), and the initial position and velocity of the satellite can be obtained by solving the TLE data into six Keplerian numbers $\sigma = (a, e, i, \Omega, \omega, v)$. Where a is the semi-major axis of the orbit, e is the orbital eccentricity, i is the orbital inclination, Ω is the ascending node right ascension, ω is the argument of perigee, and v is the true perigee angle. Figure 3 illustrates the specific meaning of the six elements of the orbit and their relationship to the Earth's inertial coordinate system. The mechanical models used for various perturbation forces are shown in Table 1.

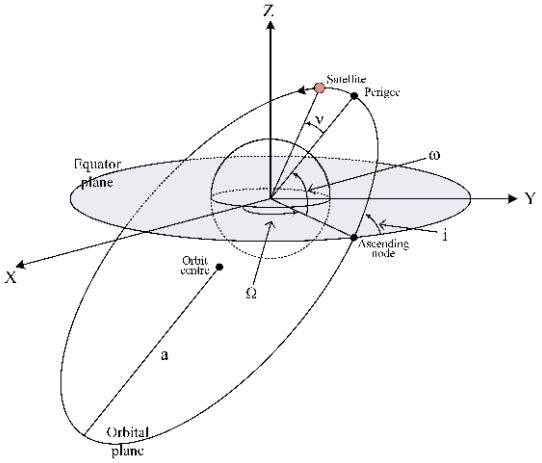


Figure 3. Relationship between Keplerian parameters and geocentric equatorial frame [9].

Table 1. The mechanical models used for various perturbation forces.

Perturbation Force	Main Impact	Model	
		LEO	GEO
Earth's non-spherical gravity	The orbital plane of LEO satellites continuously rotates, and the GEO satellites drift east-west.	EGM2008 (first 10 levels) [10]	EGM2008 (first 12 levels) [11]
N body gravity	The eccentricity of the orbit will be changed for a long time, making the orbit more and more flat, which will further increase the atmospheric perturbation and reduce the orbit height.	Sun, Moon and Other Near-Earth Planets (Ephemeris JPL.DE436)	Sun, Moon and Other Near-Earth Planets (Ephemeris JPL.DE436)
Solid tide perturbation	Change the Earth's gravity	IERS2010 [12]	Not consider
Ocean tide perturbation	Change the Earth's gravity	FES2004 [13]	Not consider
Solar pressure	Change the eccentricity of a satellite	ECOMC	ECOMC [13]
Earth albedo pressure	Change the eccentricity of a satellite	Not consider	Not consider
Atmospheric drag	Change the semi-major axis of the satellite's orbit	NRLMSISE-00	Not consider

The extracted initial parameters of the satellite orbit and the corresponding time are taken as the initial conditions of the orbit integration. The Runge–Kutta method [14] in the finite difference calculation method is used in reference [15] to numerally integrate the

variational equation of the orbital perturbation force, and the position and velocity of the satellite at any time can be calculated.

3. System Model

3.1. Design of Inter-Satellite Terahertz Communication System

For the inter-satellite terahertz communication scenario, a spaceborne terahertz communication system with an operating frequency of 310 GHz is designed. The system is consistent with the design principle of the terahertz communication system applied to the ground. At the same time, it also has the advantages of having a simple and compact structure, being easy to carry by satellites, and obvious potential for later power improvement, which is convenient for carrying out inter-satellite terahertz communication experiments. The system adopts an all-electronic method. The transmitter adopts the zero-intermediate frequency (zero-IF) transmitter of American VDI harmonic mixer, and the receiver adopts the harmonic-mixing zero-IF receiver. Assuming the same terminal configuration on each satellite, the 310 GHz satellite communication system based on VDI harmonic mixing superheterodyne transceiver is shown in Figure 4, and the system parameters are shown in Table 2.

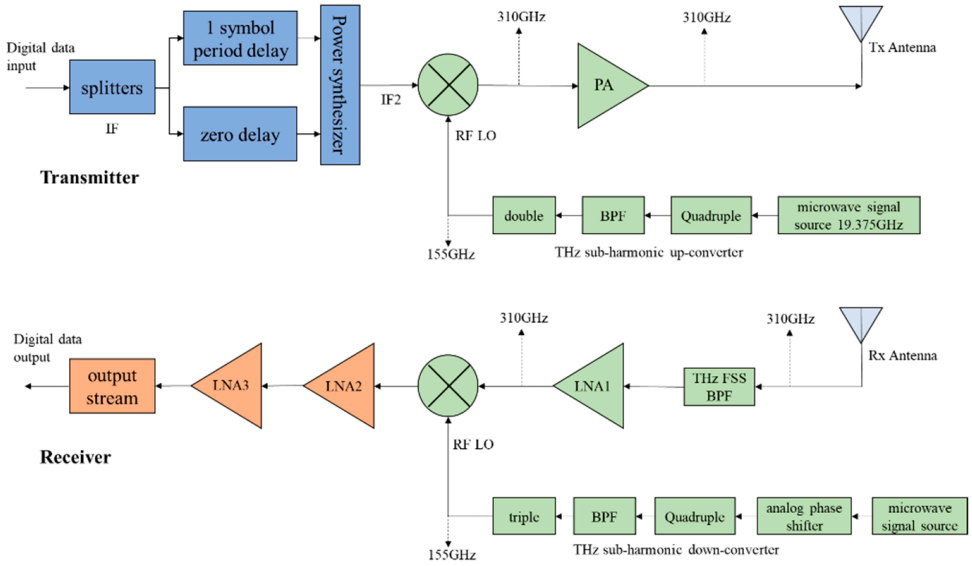


Figure 4. Block diagram of satellite terahertz communication system.

Table 2. Related parameters of satellite terahertz communication system.

Parameter	Symbol	Value	Unit
Carrier frequency	f	310	GHz
Transmit antenna gain	G_t	60	dB
Receive antenna gain	G_r	60	dB
Transmit antenna diameter	D_t	50	cm
Receive antenna diameter	D_r	50	cm
Average noise temperature	T	2700	K
Bandwidth	B	5	GHz
Transmit power	P	23	dBm
Boltzmann constant	K_B	1.381×10^{-23}	/
Modulation	/	OOK	/
Antenna feeder loss	L_k	2	dB
Polarization loss	L_i	1	dB

The microwave signal source generates a sinusoidal signal with a frequency of 19.375 GHz, which goes through a quadruple, a filter, and a doubler in sequence, and

then performs sub-harmonic mixing with the input signal IF2 when it reaches 155 GHz. A modulated signal with a center frequency of 310 GHz and a bandwidth of 5 GHz is obtained through the zero-IF up-mixing output. After passing through the power amplifier (PA), the signal is transmitted through the terahertz antenna and received by the receiver antenna. The receiving end adopts a superheterodyne mixing receiver. In order to make the received signal cover the frequency band of 307.5~312.5 GHz, the center frequency of the local oscillator (LO) of the receiver is selected as 310 GHz, and the intermediate frequency bandwidth is selected as 0~2.5 GHz. Considering the noise of the receiving IF low noise amplifier (LNA), the overall noise temperature at the receiving end is estimated to be 2700 K. In order to make the LO of the zero-IF receiver in phase with the LO of the received signal, an analog phase shifter is used to adjust the phase of the LO. Since the terahertz antenna and the terahertz front-end device are hard-connected by a waveguide, and the distance between the two is generally negligible relative to the transmission distance of thousands of kilometers between satellites, the terahertz antenna is usually not considered in the research. Instead, the transmitter, receiver and antenna of the terahertz communication system are regarded as a whole.

3.2. Noise Model

In order to study the quality of the communication link, it is necessary to calculate the signal-to-noise ratio, that is, the ratio of the useful signal power to the noise power in the signal. In order to accurately calculate the signal-to-noise ratio, it is necessary to obtain the power spectral density of the noise. Due to the unique nature of the terahertz frequency band, the terahertz wavelength is close to the size of some molecules, so many molecules in the atmosphere will resonate in the terahertz frequency band, resulting in molecular absorption, which in turn leads to frequency-selective attenuation, which also brings the channel. Additional noise, related channel noise research work has attracted extensive attention. Jornet & Akyildiz [16] analyzed the total noise in the terahertz band in the satellite-ground link, including molecular absorption noise and antenna noise. Kokkoniemi [17] studied the atmospheric noise of the communication link between the aircraft and the satellite and the thermal noise of the receiver. Studies have shown that additional atmospheric noise is introduced during molecular absorption due to the atmosphere acting as a blackbody radiator. However, this paper mainly studies the inter-satellite terahertz communication link. Therefore, considering that the noise in inter-satellite communication is mainly thermal noise at the receiver, the power spectral density of thermal noise varies with the receiver noise coefficient, and the noise power spectral density can be expressed as Equation (2).

$$N(f) = k_B T \eta(f) 10^{N_f/10} \tag{2}$$

where, $\eta(f) = \frac{hf}{k_B T[\exp(hv/k_B T)-1]}$, T is the mean temperature, f is the frequency, N_f is the noise factor, h is Planck's constant, and k_B is Boltzmann's constant.

4. Signal Attenuation Model for Inter-Satellite Terahertz Communication

4.1. Signal Attenuation Model for Inter-Satellite Terahertz Communication without Pointing Error

Considering the transmitter and receiver of the terahertz communication system as a whole, the structure of the terahertz communication link between satellites is shown in Figure 5. After the terahertz wave is generated, it is transmitted through the antenna, and the beam reaches the antenna at the receiving end after a long transmission distance. Since there is no atmosphere in space, there is no need to consider the effect of atmospheric absorption. Assuming that there is no pointing error, the received power of the inter-satellite terahertz communication system can be expressed as Equation (3).

$$P_R = P_T \cdot G_T \cdot G_R \cdot L_f \tag{3}$$

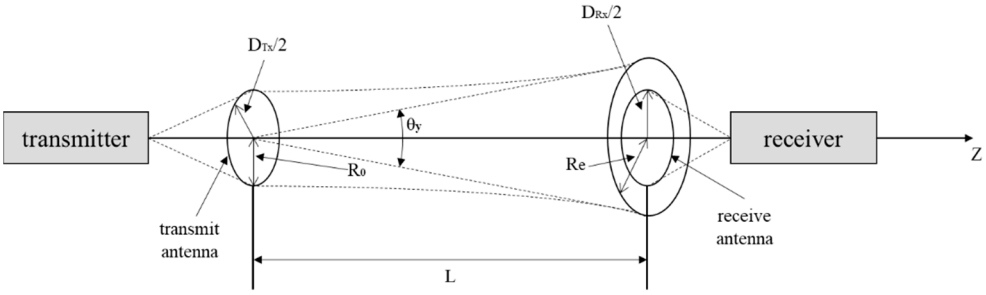


Figure 5. Inter-satellite terahertz communication link structure diagram.

Among them, P_T and P_R are the transmit power and receive power, G_T and G_R are the transmit antenna gain and receive antenna gain, respectively, and L_f are the free space loss.

In the existing link budget model, the electromagnetic signal attenuation mainly adopts the Friis equation. The Friis equation is mainly applicable to the case where the pointing error attenuation is not too serious, which is usually used in the microwave frequency bands. Considering the computational complexity in the performance analysis of terahertz communication, it is generally believed that the beams in the receiving area of the antenna are uniformly distributed [18]. However, terahertz wave has the characteristics of light-like transmission. Due to the narrow terahertz wave beam, the pointing error has a greater impact on the system, so the influence brought by the pointing error must be fully considered. In addition, when there is a large difference between the received aperture and terahertz beam radius due to other factors such as pointing error, the geometric attenuation model under the assumption of plane wave is used to calculate the received power, which will lead to a large error between the calculated received power and the actual situation. A more effective method is to add the attenuation caused by pointing error on the basis of Friis equation. In most cases, terahertz research is also based on quasi-optical theory with Gaussian beam model analysis. For example, reference [6,8,19]. In fact, most of the transmitted signals are Gaussian beams, which are unevenly distributed in the area of the receiving end. Therefore, this paper adopts the Gaussian beam model for analysis. For the Gaussian beam receiver, the terahertz wave distribution is represented by Equation (4).

$$T(r, L) = T_0 \frac{{R_0}^2}{{R_e}^2} \exp(-\frac{2r^2}{{R_e}^2}) \tag{4}$$

where, T_0 is a constant, related to the transmit power, R_0 is the beam radius of the transmitting end, r is the distance from any point in the plane at the transmitting end antenna to the center, and R_e is the effective radius of the beam reaching the receiving end, determined by Equation (5).

$$R_e = R_0 \sqrt{1 + \left(\frac{\lambda L}{\pi {R_0}^2}\right)^2} \tag{5}$$

In the formula, L is the transmission distance. The effective radius is determined by the field strength, where the field strength of the terahertz beam is $1/e^2$ at the center and obeys the hyperbolic variation law. For Gaussian beams, the beam divergence is generally expressed by the beam launch angle θ_b, which can be expressed as Equation (6).

$$\theta_b = 2\frac{dR_e}{dz} = \frac{2\frac{\lambda L}{\pi R_0}}{\sqrt{\left(\frac{\pi {R_0}^2}{\lambda}\right)^2 + L^2}} \tag{6}$$

Assuming that the transmission distance is infinite, namely $L \to \infty$, the angle between the two asymptotes of the hyperbola is the far-field divergence angle θ_y of the Gaussian beam, which can be expressed as Equation (7).

$$\theta_y = \lim_{z\to\infty} \frac{2R_e}{L} = \frac{2\lambda}{\pi R_0} \tag{7}$$

The beam launch angle and the far-field launch angle are determined by the transmitter structure of the terahertz communication system. Combined with Equations (3)–(7), the power of the transmitter and the power of the receiver can be represented by Equation (8).

$$\begin{aligned} P_T &= \int_0^{D_{Tx}} T(r,0)2\pi r dr = \frac{\pi T_0 R_0^2}{2}\left[1-\exp\left(-\frac{2{D_{Tx}}^2}{R_0^2}\right)\right] \\ P_R &= \int_0^{D_{Rx}} T(r,L)2\pi r dr = \frac{\pi T_0 R_0^2}{2}\left[1-\exp\left(-\frac{2{D_{Rx}}^2}{R_e^2}\right)\right] \end{aligned} \tag{8}$$

It is defined h as signal power attenuation, that is, the ratio of received power to transmit power. Therefore, the signal power attenuation of the inter-satellite terahertz communication system under the condition of no pointing error is Equation (9).

$$h = \frac{P_R}{P_T} = \frac{\int_0^{D_{Rx}} T(r,L)2\pi r dr}{\int_0^{D_{Tx}} T(r,0)2\pi r dr} = \frac{1-\exp\left(-\frac{2{D_{Rx}}^2}{R_e^2}\right)}{1-\exp\left(-\frac{2{D_{Tx}}^2}{R_0^2}\right)} \tag{9}$$

where, D_{Tx} and D_{Rx} are the radius of the transmitting antenna and the radius of the receiving antenna.

4.2. Signal Attenuation Model of Inter-Satellite Terahertz Communication under Pointing Error

The satellite-borne antenna is fixedly connected with the satellite constellation coordinate system, and the attitude change of the satellite will inevitably cause the antenna pointing to change. In the inter-satellite terahertz link communication process, the transmitter controls the terahertz beam to point to the receiver. Due to the influence of orbital perturbation force and other factors, both the transmitter and the receiver have pointing errors. Although the influence of the perturbation force is small, the terahertz wave will have a certain offset when it reaches the receiving end through long-distance transmission, resulting in the attenuation of the received signal power and even the communication failure.

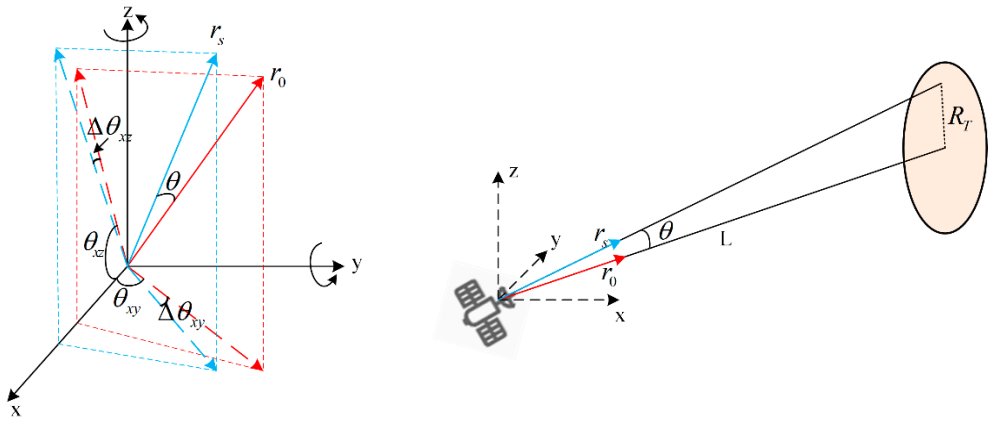
The pointing error model of satellite communication system is based on several related coordinate systems such as inertial coordinate system OXYZ, satellite body coordinate system $O_1X_1Y_1Z_1$ and antenna coordinate system $O_2X_2Y_2Z_2$ and their mutual transformations. According to the six Keplerian numbers solved by TLE, the position of the satellite in the inertial coordinate system can be obtained by Equation (10).

$$\begin{bmatrix} X \\ Y \\ Z \end{bmatrix} = \frac{a\left(1-e^2\right)}{1+e\cos f}\begin{bmatrix} \cos\Omega\cos u - \sin\Omega\sin u\cos i \\ \sin\Omega\cos u + \cos\Omega\sin u\cos i \\ \sin u\cos i \end{bmatrix} \tag{10}$$

Since this paper mainly considers the pointing error caused by satellite perturbation, in order to simplify the calculation, this paper assumes that there is no assembly error, and the antenna coordinate system coincides with the satellite body coordinate system. Define the angle between the inertial coordinate system and the satellite body coordinate system as α, β, γ, then the transformation matrix can be represented by Equation (11).

$$A = \begin{bmatrix} \cos\alpha\cos\beta & \sin\alpha\cos\beta & -\sin\beta \\ -\sin\alpha\cos\gamma + \cos\alpha\sin\beta\sin\gamma & \cos\alpha\cos\gamma + \sin\alpha\sin\beta\sin\gamma & \sin\alpha\cos\beta \\ \sin\alpha\sin\gamma + \cos\alpha\sin\beta\cos\gamma & \sin\alpha\sin\beta\cos\gamma - \cos\alpha\sin\gamma & \cos\gamma\cos\beta \end{bmatrix} \tag{11}$$

In the antenna coordinate system, the azimuth angle θ_{xy} and the elevation angle θ_{xz} of the transmitter are shown in Figure 6a, and the rotation direction along the arrow is the positive direction. Assuming that the pointing vector of the transmitter in the antenna coordinate system is $\vec{r} = (x, y, z)$, the azimuth angle θ_{xy} and the elevation angle θ_{xz} of the transmitter can be described as Equation (12).



(**a**) (**b**)

Figure 6. Schematic diagram of the transmitting signal of the terahertz wave transmitter: (**a**) the change of the signal beam emission angle in the antenna coordinate system; (**b**) the change of the signal beam emission direction.

$$\theta_{xy} = \arctan\frac{y}{x},\ \theta_{xz} = \arctan\frac{z}{x} \tag{12}$$

Figure 6b shows the unit vector r_0 of the terahertz wave emission direction and the unit vector r_s of the terahertz wave emission direction under the influence of pointing error. The angle θ between the pointing vector r_0 without pointing error and the pointing vector r_s with pointing error is the pointing error angle. Assuming that the perturbed position of the satellite receiving end is $r_1(x_1, y_1, z_1)$ and the offset displacement is $\Delta r_1(\Delta x_1, \Delta y_1, \Delta z_1)$, the azimuth pointing error angle $\Delta\theta_{xy}$, and the pitch pointing error angle $\Delta\theta_{xz}$ can be expressed as Equation (13).

$$\begin{gathered}
\Delta\theta_{xy} = \begin{bmatrix} \frac{\cos^2\theta_{xy}}{x_0} & \frac{-\sin^2\theta_{xy}}{y_0} \end{bmatrix} \begin{bmatrix} \Delta y_0 \\ \Delta x_0 \end{bmatrix} \\
\Delta\theta_{xz} = \begin{bmatrix} \frac{-\tan\theta_{xz}\cdot x_0}{x_0^2+y_0^2+z_0^2} & \frac{-\tan\theta_{xz}\cdot y_0}{x_0^2+y_0^2+z_0^2} & \frac{\cos\theta_{xz}}{\sqrt{x_0^2+y_0^2+z_0^2}} \end{bmatrix} \begin{bmatrix} \Delta x_0 \\ \Delta y_0 \\ \Delta z_0 \end{bmatrix} \\
\begin{bmatrix} \Delta x_0 \\ \Delta y_0 \\ \Delta z_0 \end{bmatrix} = A \begin{bmatrix} \Delta x_1 \\ \Delta y_1 \\ \Delta z_1 \end{bmatrix}
\end{gathered} \tag{13}$$

The pointing error angle is decomposed into the azimuth pointing error angle $\Delta\theta_{xy}$ and the pitch pointing error angle $\Delta\theta_{xz}$, and the pointing error angle can be expressed as Equation (14).

$$\theta = \sqrt{\left(\cos\theta_{xz}\Delta\theta_{xy} + \sin\theta_{xy}\sin\theta_{xz}\Delta\theta_{xz}\right)^2 + \cos^2\theta_{xy}\Delta\theta_{xz}{}^2} \tag{14}$$

At the receiving end, the terahertz beam offset R_T is expressed as $R_T = L\theta$. Assuming that the receiving end is a circular surface, affected by the pointing error, there will be a certain misalignment between the beam center at the receiving end and the center of the

circular surface. The beam trajectory change of the receiving end caused by the pointing error is shown in Figure 6.

As shown in Figure 7, a plane rectangular coordinate system is established with the center of the receiver receiving plane as the origin, and under the condition of pointing error, the terahertz beam distribution at the receiving end is expressed by Equation (15).

$$T(r - R_T, L) = T_0 \frac{{R_0}^2}{{R_e}^2} \exp\left(-\frac{2(r - R_T)^2}{{R_e}^2}\right) \tag{15}$$

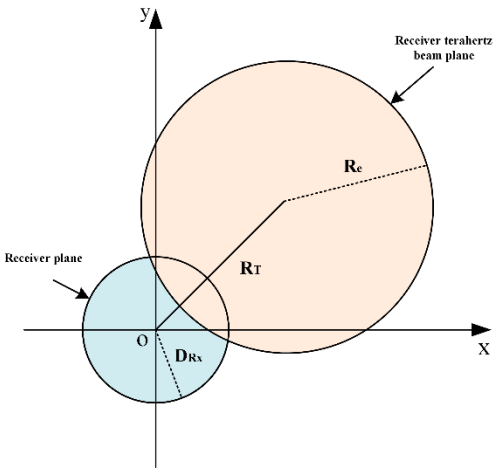


Figure 7. Schematic diagram of beam trajectories caused by pointing errors in the receiver plane.

$h_{err}(\theta)$ is the signal power attenuation considering the pointing error, expressed by Equation (16), which is a function of the pointing error angle. The larger the value of $h_{err}(\theta)$, the smaller the influence of the pointing error; the smaller the value of $h_{err}(\theta)$, the greater the influence of the pointing error.

$$h_{err}(\theta) = \frac{P_R(\theta)}{P_T} = \frac{\int_{x_1}^{x_2} \int_{\sqrt{{D_{Rx}}^2 - (x - L\Delta\theta_{xy})^2} + L\Delta\theta_{xz}}^{\sqrt{{R_e}^2 - x^2}} T(x,y)dxdy}{\int_{-D_{Rx}}^{D_{Rx}} \int_{-\sqrt{{D_{Rx}}^2 - x^2}}^{\sqrt{{D_{Rx}}^2 - x^2}} T(x,y)dxdy} \tag{16}$$

In the Equation (16), $0 \le h_{err}(\theta) \le 1$, when $h_{err}(\theta)$ is equal to 1, it means that there is no pointing error, and when $h_{err}(\theta)$ is equal to 0, it means that the receiving end cannot receive any signal due to the extremely large pointing error. x_1 and x_2 can be solved by Equation (17).

$$\begin{cases} x^2 + y^2 = {R_e}^2 \\ (x - L\Delta\theta_{xy})^2 + (y - L\Delta\theta_{xz})^2 = {r_e}^2 \end{cases} \tag{17}$$

Since it is difficult to solve the integral solution of signal power attenuation in the plane rectangular coordinate system, considering that the actual receiving area of the receiving end is a circle, the integral calculation is carried out in the polar coordinate system, and Equation (18) can be obtained, that is, the analytic solution of signal power attenuation.

$$h_{err}(\theta) = \frac{P_R(\theta)}{P_T} = \begin{cases} \dfrac{\exp\left(-\frac{2R_T^2}{R_e^2}\right) - \exp\left(-\frac{8D_{Rx}^2}{R_e^2(2-R_T)^2}\right) + \frac{\sqrt{2\pi}R_T}{R_e}\left[erf\left(\frac{\sqrt{2}R_T}{R_e}\right) + erf\left(\left|\frac{2\sqrt{2}D_{Rx}}{(2-R_T)R_e}\right|\right)\right]}{1 - \exp\left(-\frac{2{D_{Tx}}^2}{R_0^2}\right)}, D_{Rx} > R_T \\ \dfrac{\exp\left(-\frac{2R_T^2}{R_e^2}\right) - \exp\left(-\frac{8D_{Rx}^2}{R_e^2(2-R_T)^2}\right) + \frac{\sqrt{2\pi}R_T}{R_e}\left[erf\left(\frac{\sqrt{2}R_T}{R_e}\right) - erf\left(\left|\frac{2\sqrt{2}D_{Rx}}{(2-R_T)R_e}\right|\right)\right]}{1 - \exp\left(-\frac{2{D_{Tx}}^2}{R_0^2}\right)}, D_{Rx} \le R_T \end{cases} \tag{18}$$

5. Results

Assume that the diameter of the transmitter and receiver of the inter-satellite terahertz communication system is 0.5 m, the carrier frequency is 180 GHz, and the link transmission distance is 100 km. In this scenario, through the simulation of the above models, the relationship between the pointing error angle, beam radius at the transmitter and signal power attenuation is obtained, as shown in Figure 8.

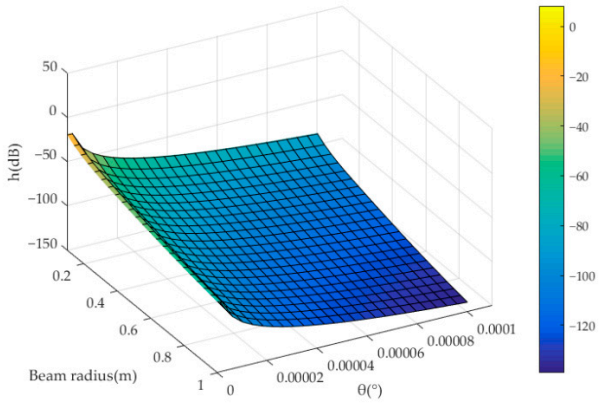


Figure 8. The relationship between pointing error angle, beam radius at the transmitting end, and signal power attenuation.

It can be seen from Figure 8 that when the pointing error angle and the beam radius of the transmitting end are different, as the beam radius increases, the signal power attenuation increases continuously. As the pointing error angle increases, the signal power attenuation also increases. In addition, as the beam radius continues to increase, the signal power attenuation changes more and more slowly with the pointing error. This shows that when the beam radius becomes larger, the effective radius of the beam reaching the receiving end also increases, and the power attenuation caused by the pointing error increases relatively slowly.

In this section, STK software is used to simulate the motion scenarios of low-orbit satellites and geostationary satellites affected by perturbation forces in space. The variation of the pointing error angle with the satellite running time is analyzed. The relationship between the pointing error angle and the azimuth and elevation angles of the transmitter is studied. Taking a low-orbit satellite and a geostationary satellite as an example, the pointing error angle, signal power attenuation, and signal-to-noise ratio of the terahertz communication system are simulated based on the satellite perturbation model and the inter-satellite terahertz communication link model. The effect of pointing error on the inter-satellite terahertz communication link is analyzed by simulation.

5.1. Pointing Error Angle Simulation

Taking a low-orbit satellite and a geostationary orbit satellite as an example, the motion scene of the low-orbit satellite and the geostationary orbit satellite affected by the perturbation force in space is simulated by STK software. The TLE information of low-orbit satellites and geostationary-orbit satellites is given in Table 3.

Table 3. Satellite TLE Information.

Parameter	LEO	GEO
Semimajor axis (km)	686	35797
Eccentricity	1.06×10^{-3}	2.25×10^{-4}
Inclination (deg)	98.1268	0.1129
RAAN (deg)	354.3541	80.757
Argument of Perigee (deg)	65.62	125.98
True Anomaly (deg)	0	19.22

According to the satellite perturbation model in Section 1, the six Keplerian numbers are solved through the TLE data to obtain the initial position and velocity of the satellite. The number of orbital elements of the satellite at any time, and finally the azimuth angle, pitch angle, and pointing error angle of the transmitter are solved according to the inter-satellite terahertz link model. In this paper, through the co-simulation of matlab and stk, the calculated orbital elements of the satellite at any time are input into stk through matlab, and stk is used to simulate the inter-satellite terahertz communication scene. The scene parameters are set as follows: the scene time is from 04:00:00 on 12 July 2022 to 04:00:00 on 14 July 2022, see Figure 9 for the scene.

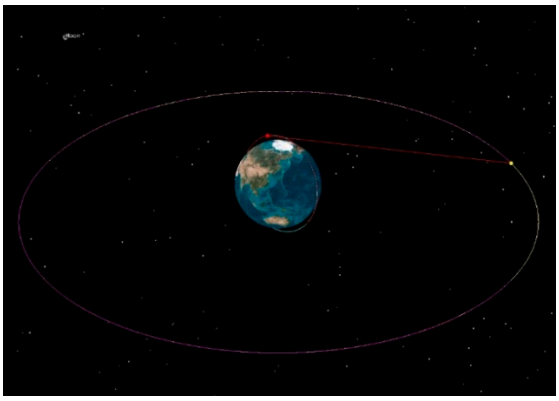
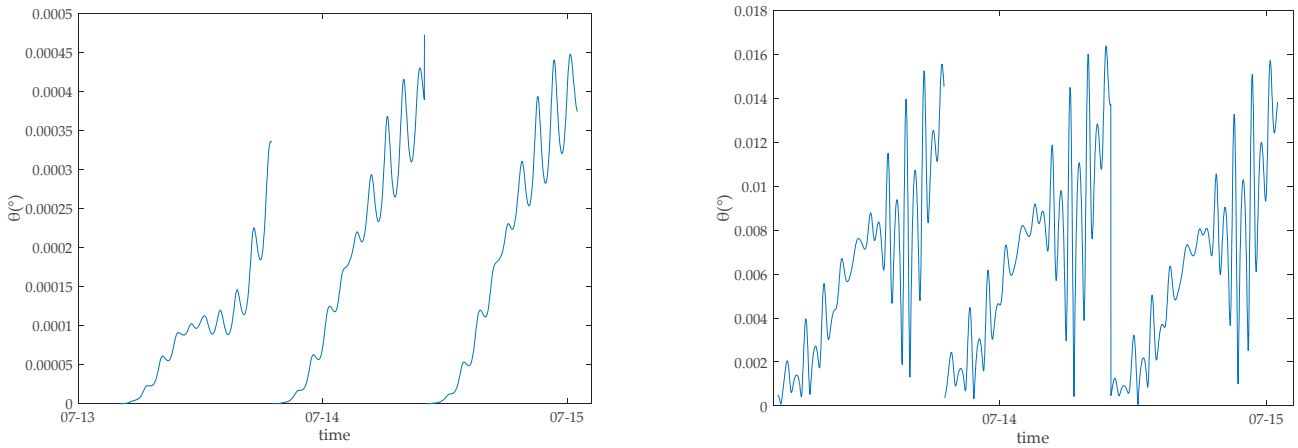


Figure 9. Schematic diagram of stk simulation scene.

The low-orbit satellites and geostationary-orbit satellites will be affected by various perturbation forces during operation, resulting in orbital deviations. If the perturbation forces are allowed to act on the satellites, the satellite orbits will change dramatically, resulting in huge pointing errors. Therefore, when the satellite passes through the ground station, the ground station will send an orbit control command to the satellite to correct the error of the satellite deviating from the orbit, so that it can return to the predetermined orbit and effectively control the pointing error. In this paper, it is assumed that every time the satellite passes through the ground station, an orbit adjustment is performed. For the uplink terahertz communication link of LEO-GEO, the antenna of the low-orbit satellite is pointed as the transmitting direction, and the antenna of the geostationary orbit satellite is responsible for receiving. For the downlink terahertz communication link of GEO-LEO, the antenna of the geostationary orbit satellite is pointed to the transmitting direction, and the low-orbit satellite antenna is responsible for receiving. According to the satellite perturbation model and the pointing error model, the pointing errors of the uplink and downlink are calculated, respectively, and the variation of the pointing error angle with time is obtained, as shown in Figure 10.

It can be seen from Figure 10 that with the increase of time, in the case of no orbit adjustment, the pointing error angles of the uplink and the downlink have an increasing trend as a whole, and the maximum is 0.01638°. It can also be seen that the pointing error angle of the downlink is much larger than that of the uplink, indicating that the influence of the perturbation force on the low-orbit satellite is greater than that of the geostationary orbit satellite. In addition, it is obvious from Figure 10 that the variation of the pointing error angle with time has a periodicity, which is likely to be related to the periodic motion of the low-orbit satellite, and with the increase of the number of operating cycles of the low-orbit satellite. The magnitude and variation of the pointing error angle are also gradually increasing, probably due to the cumulative effect of the perturbation force on the satellite with the increase of time. If the orbit control is not performed when the satellite passes through the Earth station, the pointing error angle will become larger and larger, which will have an incalculable impact on the inter-satellite terahertz communication system, and even the communication will be interrupted. It can be seen from Figure 11 that the azimuth angle has little influence on the pointing error angle, and the pitch angle has a

great influence on the pointing error angle. When the pitch angle is close to 90 degrees, the pointing error angle increases sharply. In addition, when the azimuth and pitch angles are equal in magnitude, the pointing error angle is the smallest.



(**a**) (**b**)

Figure 10. Variation of pointing error angle caused by satellite orbit perturbation with time: (**a**) uplink terahertz communication link for LEO-GEO; (**b**) downlink terahertz communication link for GEO-LEO.

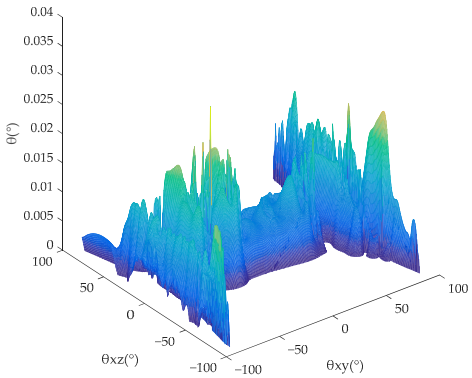


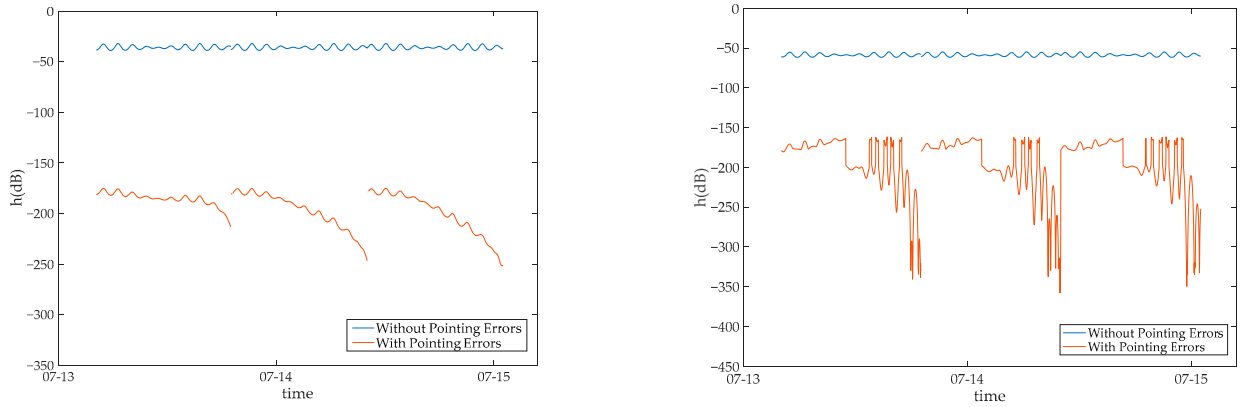
Figure 11. Relationship between transmitter pitch angle, azimuth angle and pointing error angle.

5.2. Signal Power Attenuation Simulation

Based on the designed satellite terahertz communication system and inter-satellite terahertz communication scenario, the power attenuation of the inter-satellite terahertz communication signal is calculated and simulated according to the value of the calculated pointing error angle, and it can be obtained signal power attenuation as a function of time. Assuming that the radius of the receiving antenna is 0.5 m, the signal power attenuation under the condition of no pointing error and under the condition of pointing error is obtained through simulation, as shown in Figure 12.

It can be seen from Figure 12 that, under the condition of no pointing error, the signal power attenuation is comprised between −40 and −60 dB, which is relatively stable. Under the condition of pointing error, the signal power attenuation is as periodic distribution as the pointing error angle. As the pointing error angle increases, the signal power attenuation also increases. The minimum value of uplink signal power attenuation is −175.5 dB, the maximum value is −248.4 dB, the minimum value of downlink signal power attenuation is −164.1 dB, and the maximum value is −357.8 dB. After the attitude adjustment of the ground station, the signal power attenuation decreases rapidly. It can be seen from the comparison that the signal power attenuation caused by the pointing

error is very large. If the attitude control adjustment is not performed, it is likely to cause communication interruption.



(**a**) (**b**)

Figure 12. Signal power attenuation with no pointing error and with pointing error: (**a**) uplink terahertz communication link for LEO-GEO; (**b**) downlink terahertz communication link for GEO-LEO.

5.3. Signal to Noise Ratio Simulation

According to the pointing error model and the noise model, considering the path loss, the signal-to-noise ratio at the receiver can be expressed as Equation (19).

$$SNR = \int_B \frac{X(f)PL(f,l)h_{err}(\theta)}{N(f)}df \tag{19}$$

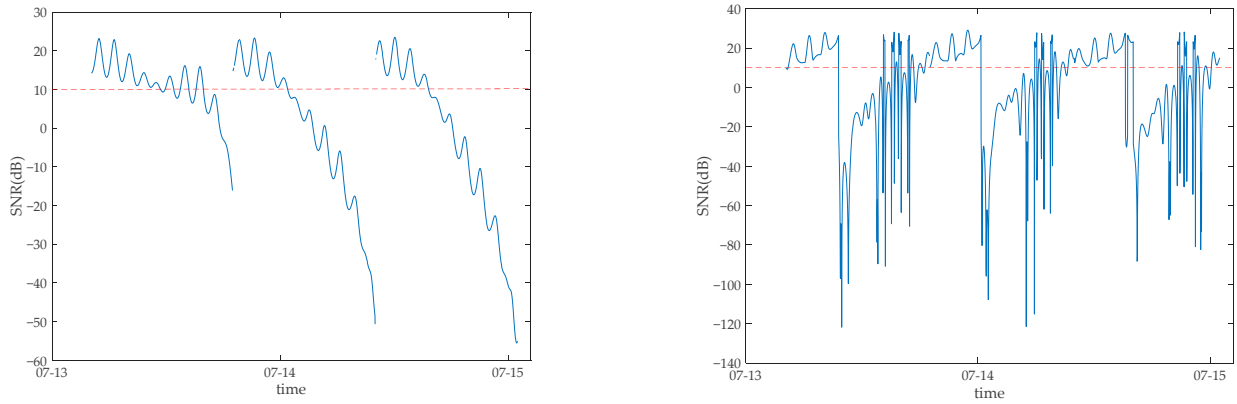
Among them, B is the bandwidth, $X(f)$ is the power spectral density of the transmitted signal, $PL(f,l)$ is the total path attenuation loss, including free space loss and antenna gain, which can be expressed as $PL(f,l) = L_f + G_R + G_T$. L_f represents the free space loss, which can be written as Equation (20).

$$L_f = 20\lg f(\text{GHz}) + 20\lg d(\text{km}) + 92.4\text{dB} \tag{20}$$

For a given inter-satellite terahertz communication scenario, the signal-to-noise ratio is shown in Figure 13. In the terahertz frequency band, the maximum signal-to-noise ratio of the uplink can reach 23.47 dB, and the maximum signal-to-noise ratio of the downlink can reach 29.04 dB. With the increase of time, the influence of the orbital perturbation force on the satellite is increasing, and the signal-to-noise ratio of the inter-satellite communication link tends to decrease as a whole. Due to the long distance of satellite communication and the limitation of the current development level of terahertz power devices, the signal-to-noise of terahertz communication system is low. Therefore, we assume that the lowest signal-to-noise that can satisfy the normal communication of terahertz communication system is 10 dB. We define the operation period of the satellite as starting from the current satellite passing through the ground station to the end of the next satellite passing through the ground station. It can be seen from Figure 13 that in the second half of the satellite operation cycle, the system's signal-to-noise ratio cannot meet the minimum signal-to-noise ratio requirements, which will lead to a sharp increase in the bit error rate, reduced notification quality and even communication interruption.

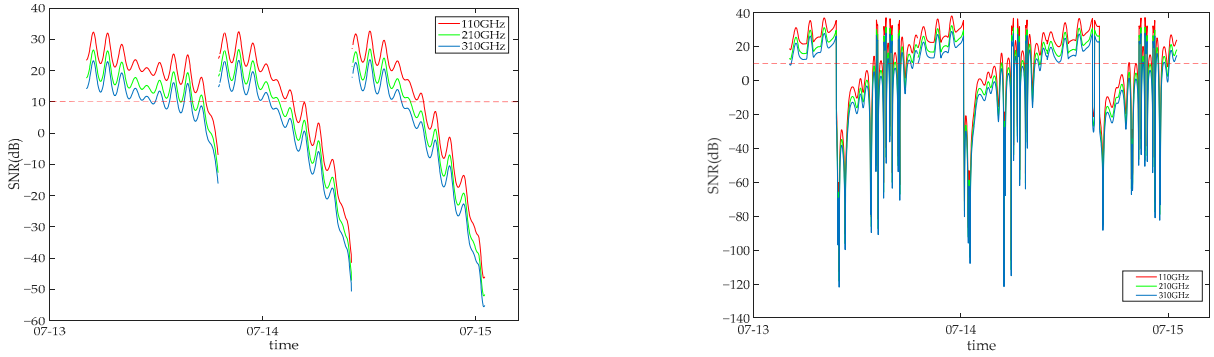
The communication link is greatly affected by the communication frequency. The lower the frequency, the higher the signal-to-noise ratio of the link and the better the communication quality. It can be seen from Figure 14 that for the same pointing error angle at the same time, when the frequency is higher, the interruption probability of the inter-satellite terahertz communication link is greater, and the pointing error of the transmitter also has a greater impact on the communication quality of the terahertz communication

system. Therefore, the higher the operating frequency of the inter-satellite terahertz communication system, the higher the demand for pointing error accuracy, and the slight perturbation of the satellite may have a greater impact on the communication system.



(**a**) (**b**)

Figure 13. Variation of signal-to-noise ratio with time in inter-satellite terahertz communication system: (**a**) uplink terahertz communication link for LEO-GEO; (**b**) downlink terahertz communication link for GEO-LEO.



(**a**) (**b**)

Figure 14. Variation of signal-to-noise ratio with time at different communication frequencies in inter-satellite terahertz communication system: (**a**) uplink terahertz communication link for LEO-GEO; (**b**) downlink terahertz communication link for GEO-LEO.

6. Conclusions

Due to the particularity of its location in the terahertz frequency band, satellite terahertz communication technology has become one of the important technical means to achieve high-speed, large-capacity, and long-distance communication in space. Since the terahertz beam is narrow and the satellite is affected by the perturbation force in different directions in space, in order to achieve high-speed, large-capacity, and long-distance communication, it is necessary to study the pointing performance of the inter-satellite terahertz communication system. In this paper, the perturbation model of satellites in different orbits is established by analyzing the specific perturbation force and the specific direction of the antenna during the orbit of the satellite, and the inter-satellite terahertz communication link with and without pointing error is analyzed. Finally, a satellite terahertz communication system is designed, and the satellite perturbation orbit, pointing error angle, signal power attenuation and system signal-to-noise ratio are simulated and analyzed according to two hypothetical satellites. The simulation results show that the pointing error angle increases periodically with the increase of the satellite's running time. Therefore, it is necessary to

take measures to suppress the influence of the perturbation force on the satellite to reduce the pointing error. By comparing the signal power attenuation without pointing error and the signal power attenuation with pointing error, it is found that the signal power attenuation caused by the pointing error reaches more than 100 dB. However, the current gain of high-gain terahertz antennas is mostly at the level of 60 dB, it is difficult to compensate for the huge loss caused by pointing error. Under the same pointing error, the higher the frequency, the lower the signal-to-noise ratio of the communication system and the worse the communication quality. This is also an important limiting factor for the development of current terahertz communication systems in the low terahertz frequency band. If the attitude control of the satellite is not carried out, signal distortion, communication quality degradation and even communication interruption will occur in a very short period of time.

Author Contributions: Conceptualization, Y.H. and C.M.; methodology, Y.H. and C.M.; software, C.M.; validation, Y.H. and C.M.; formal analysis, Y.H. and C.M.; investigation, Y.H.; resources, Y.H.; data curation, C.M.; writing—original draft preparation, C.M.; writing—review and editing, Y.H.; visualization, C.M.; supervision, Y.H.; project administration, Y.H.; funding acquisition, Y.H. All authors have read and agreed to the published version of the manuscript.

Funding: The national key research and development program sponsored this work under grant number 2019YFB1803201.

Institutional Review Board Statement: Not applicable.

Informed Consent Statement: Not applicable.

Data Availability Statement: The data presented in this study are available from the corresponding author upon reasonable request.

Conflicts of Interest: The authors declare no conflict of interest.

References

1. Kukutsu, N.; Hirata, A.; Kosugi, T.; Takahashi, H.; Nagatsuma, T.; Kado, Y.; Nishikawa, H.; Irino, A.; Nakayama, T.; Sudo, N. 10-Gbit/s Wireless Transmission Systems Using 120-GHz-Band Photodiode and MMIC Technologies. In Proceedings of the 2009 Annual IEEE Compound Semiconductor Integrated Circuit Symposium, Greensboro, NC, USA, 11–14 October 2009.
2. Kallfass, I.; Antes, J.; Lopez-Diaz, D.; Wagner, S.; Tessmann, A.; Leuther, A. Broadband Active integrated circuits for Terahertz communication. In Proceedings of the 2012 18th European Wireless Conference, Poznan, Poland, 18–20 April 2012.
3. Harter, T.; Füllner, C.; Kemal, J.N.; Ummethala, S.; Steinmann, J.L.; Brosi, M.; Hesler, J.L.; Bründermann, E.; Müller, A.-S.; Freude, W.; et al. Generalized Kramers–Kronig receiver for coherent terahertz communications. *Nat. Photonics* **2020**, *14*, 601–606. [CrossRef]
4. Chen, Z.; Zhang, B.; Zhang, Y.; Yue, G.R.; Fan, Y.; Yuan, Y. 220 GHz outdoor wireless communication system based on a Schottky-diode transceiver. *IEICE Electron. Express* **2016**, *13*, 20160282. [CrossRef]
5. Niu, Z.Q.; Zhang, B.; Wang, J.L.; Liu, K.; Chen, Z.; Yang, K.; Zhou, Z.; Fan, Y.; Zhang, Y.H.; Ji, D.F.; et al. The research on 220GHz multicarrier high-speed communication system. *China Commun.* **2020**, *17*, 131–139. [CrossRef]
6. Nie, S.; Akyildiz, I.F. Channel Modeling and Analysis of Inter-Small-Satellite Links in Terahertz Band Space Networks. *IEEE Trans. Commun.* **2021**, *69*, 8585–8599. [CrossRef]
7. Bai, L.T.; Zhu, Z.B.; Li, X.J. Analysis of THz space communication link based on STK. In Proceedings of the 2021 3rd International Conference on Electronic Engineering and Informatics, Dali, China, 18–20 June 2021.
8. Ding, Y.M.; Shi, X.; Gao, S.; Wu, H.; Zhang, R. Analysis of tracking-pointing error and platform vibration effect in inter-satellite terahertz communication system. In Proceedings of the 2017 Chinese Automation Congress, Jinan, China, 20–22 October 2017.
9. Kahraman, Y.E.; Akbulut, A. Investigation of the Effects of Pointing Errors on Optical Intersatellite Links Using Real Orbital Data. In Proceedings of the 2021 8th International Conference on Electrical and Electronics Engineering, Antalya, Turkey, 9–11 April 2021.
10. Yang, Z.T.; Liu, J.; Liu, L. Improved method of orbit analytical solution and its application. *Syst. Eng. Electron.* **2020**, *42*, 427–433. [CrossRef]
11. Zhao, D.F.; Zhang, H.W. A study of the effect of lunar gravitational perturbation on high orbit satellites. *J. Navig. Position.* **2021**, *9*, 33–40. [CrossRef]
12. Song, C.F.; Zhu, L.Z.; Zhao, Z.H.; Zhang, H.W. Numerical Analysis of Perturbation Forces of GPS and BDS Satellites. *Geomat. Spat. Inf. Technol.* **2016**, *39*, 43–46.

13. Sun, G.J.; Zhao, L.; Li, H.; Wang, R.L.; Lu, X.T. Applicability analysis of empirical solar radiation pressure models for Beidou-3 MEO satellite orbit determination. In Proceedings of the 2022 13th China Satellite Navigation Conference, Beijing, China, 25–27 May 2022.
14. Zhang, Y.Q. High-precision satellite orbit prediction algorithm design and software development. *Harbin Inst. Technol.* **2021**. [CrossRef]
15. He, B.Y.; Jiang, Y.; Li, H. N Perturbed orbit offset deployment and configuration maintenance of two typical heterogeneous constellations. *Aerosp. Control* **2022**, *40*, 41–46.
16. Jornet, J.M.; Akyildiz, I.F. Channel modeling and capacity analysis for electromagnetic wireless nanonetworks in the terahertz band. *IEEE Trans. Wirel. Commun.* **2011**, *10*, 3211–3221. [CrossRef]
17. Kokkoniemi, J.; Jornet, J.M.; Petrov, V.; Koucheryavy, Y.; Juntti, M. Channel Modeling and Performance Analysis of Airplane-Satellite Terahertz Band Communications. *IEEE Trans. Veh. Technol.* **2021**, *70*, 2047–2061. [CrossRef]
18. Liu, X.G.; Liu, M.; Mao, Z.Y.; Xu, J.W.; Hu, H. Analysis of geometric attenuation model of gaussian beam under pointing error. *Acta Electron. Sin.* **2021**, *49*, 1893–1899.
19. Yu, J.S.; Chen, X.D. *Millimeter and Submillimeter Wave Quasi-Optical Technology*; Beijing University of Posts and Telecommunications Press: Beijing, China, 2010.